

# A new Fuel Cell converter topology For Bidirectional Power Flow between the Electric Vehicle and DC or AC Grid

SANDHYA.P<sup>1</sup>.D.POMYA<sup>2</sup>

M.TECH (Student scholar)Anurag Group of Institutions (autonomous university,kodad, Telangana, India.

Assistant professor Anurag Group of Institutions (autonomous university,kodad, Telangana, India

Email:- [sandhyap244@gmail.com](mailto:sandhyap244@gmail.com)

[Pomya.naik@gmail.com](mailto:Pomya.naik@gmail.com)

**Abstract**—Electric vehicles (EVs) are needed in densely populated urban areas to reduce air pollution. Battery chargers are needed to supply dc voltage to charge the high-energy battery packs used in EVs. This paper presents a fuel cell powered integrated traction machine and converter topology that has bidirectional power flow capability between an electric vehicle and the dc or ac supply or grid. These operations are in addition to the vehicle traction mode of operation. Desired features for EV battery chargers such as minimum volume, low cost, high efficiency, and high reliability are fully matched by means of the proposed solution. The concept has been analyzed with finite-element- coupled simulation with dynamic analysis software. The interleaving technique has been used with the inductors to share the current and reduce the converter switching stresses.

**Keywords**—Bidirectional converter, electric vehicle, integrated converter, machine inductance, vehicle-to-grid (V2G).

## I. INTRODUCTION

THE multipurpose use of the power electronic converter in the drivetrain of an electric vehicle has become an interesting topic for minimizing the system size, weight, and cost. The weight and size of the converter are challenging issues in the case of on-board chargers which otherwise provides the flexibility of charging the vehicle anywhere. The vehicle is not driven during the period of charging, and hence, the traction motor and inverter of the powertrain can be used as an integral part of the converter. The windings of the traction motor can serve as the inductors of the power converter along with power devices of the traction inverter to transfer power. The power converter of the electric vehicle can draw power from the grid when it requires, and also can deliver power to the grid in the peak time when the grid needs power. During a significant part of the day, most vehicles remain idle in the parking lot when the integrated power converter can use the traction motor and its drive to transfer power to the grid.

Several research activities for integrating the battery charging system with the traction drive have been reported in [1] and [2].

In one approach, the traction motor windings have been used as the inductors for the converter to develop the charging system without any additional component [3]. The three-phase

supply is connected with each phase of the machine and the battery

Is always connected to the dc bus. The research showed the use of a poly-phase machine for the charger. Other topologies have been used for battery charging systems with traction motor windings used as filter components [4]–[6]. An on-board integrated charger has been proposed with reconfiguration of the stator windings of a special electric machine in [7]. A charger is developed for the electric scooter, where interior permanent magnet traction motor is used for charging with power factor correction [8]. The interleaving technique is another interesting approach used in designing dc–dc converters for reduced switching stresses and increased efficiency [9]–[11]. The approach reduces the size and power rating of the converter passive components. Low EMI and low stress in the switches can be expected from the interleaved converter phase legs [11].

In this paper, a fuel cell powered integrated motor converter is proposed that can be used as the traction motor drive, a battery charger, and a power converter to transfer energy from vehicle-to-grid (V2G) through reconfiguration of the inverter topology using relays or contactors. The traction inverter with the proposed reconfiguration method can also transfer power from the vehicle to a dc grid and from a dc grid to the vehicle using the traction motor windings with the appropriate relay settings. The three phase machine windings and the three inverter phase legs can be utilized with an interleaved configuration to distribute the current and reduce the converter switching stresses. The battery voltage is increased in the boost mode to an output reference voltage level within the limits of the machine ratings. A soft starter method using PWM control has been used to reduce the starting current overshoot when connecting to a dc grid.

The proposed converter system can also be used for transferring power between a single-phase ac grid and the vehicle in either direction without any extra component. The rated conditions of the motor and utility interface are quite similar. The inverter is able to regulate the motor phase current in the entire speed range. When changing from the motor control mode to ac grid connected mode of operation, the back EMF voltage is replaced with the grid voltage. Considering the operating conditions with the grid, motor inductance would be enough to handle the grid connected

modes of operation. Also, in the blocked rotor condition, motor magnetizing inductance dominates and contributes to the phase inductance significantly. For high enough inductance required in case of ac grid, the rotor can be locked which will give high inductance in the blocked Rotor condition. In the charging mode, the machine is thermally stable with no electromechanical power flow through the air gap of the machine. The machine ratings are within limits in all the operating modes as there is only electric loading, and no magnetic loading except during traction operation. The current limit is higher in converter modes compared to the traction mode current limit.

This paper presents the analysis, design, and experiments of the integrated traction drive and power converter for electric/hybrid vehicle applications. The electric machine has been analyzed using coupled simulation of finite-element and dynamic analysis software. The power converter and controller have been modeled using Simulink. The proposed converter reconfiguration method is advantageous for reducing the size and component of the electric power train while providing bidirectional power flow capability with connections to either dc or ac supplies.

## II. CONVERTER TOPOLOGY

Different types of topologies have been developed for electric vehicles for battery charging and bidirectional power flow between the battery and the power supply. However, the traction inverter uses the standard six-switch configuration that has elements of the various power converter topologies. The proposed converter topology utilizing the traction inverter along with the switches used for reconfiguration is shown in Fig. 1(a) and (b) shows the detailed switch or relay arrangements required for different modes of operations. Several different configurations can be obtained by appropriate positioning of the switches, which results in a novel methodology for bidirectional power transfer between a vehicle battery and dc or ac grid. Including the use of the topology as the traction inverter during vehicle operation this power converter can be operated in five different modes: 1) power flow from the battery to the dc grid, 2) power flow from the dc grid to the battery, 3) traction mode, 4) power flow from the battery to single-phase ac grid and 5) power flow from a single-phase ac grid to the battery.

The reconfiguration switches can be realized with relays or Contactors depending on the ratings of the currents. Those relays and contactors are controlled in a coordinated way to accommodate the different modes of use. The size of the contactor has to be accommodated based on the current rating chosen.

The switches will be controlled for the different modes of operation using State 1 and State 2 conditions given in Table 1. Fig. 1(b) shows the details of the configuration in the routing box with the switches which relates to the operations of the switches according to Table I. The terminal numbers

are shown in Fig. 1(b) inside the switches which are changed to different positions for the different configurations.

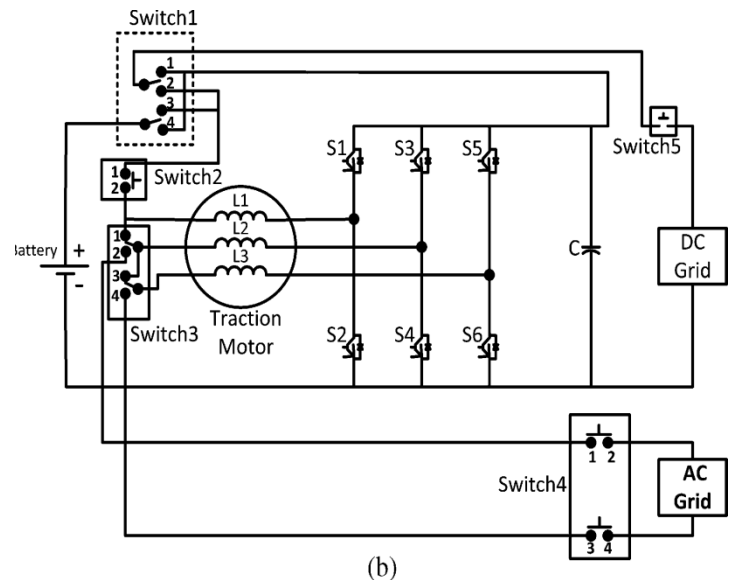
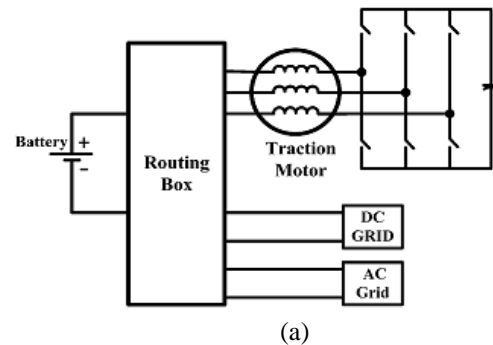


Fig. 1. Converters with switches capable of interfacing with both ac and dc grid (a) combined (b) details.

**TABLE 1**  
**SWITCH POSITIONS AND CONVERTER STATES**

with the three inductances and three legs of the converter; for G2V boost operation, the interleaved technique can be applied on the dc grid side to reduce the switching

Switch	State 1	State 2
Switch 1	Pole positions: 1 and 3	Pole positions: 2 and 4
Switch 2	1 and 2 disconnected	1 and 2 connected
Switch 3	Pole positions: 1 and 3	Pole positions: 2 and 4
Switch 4	1 and 2, and 3 and 4 disconnected	1 and 2, and 3 and 4 connected
Switch 5	1 and 2 disconnected	1 and 2 connected

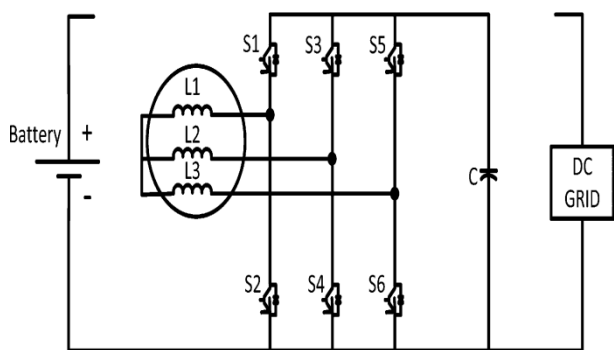


Fig.2.circuit with all switches in state 2

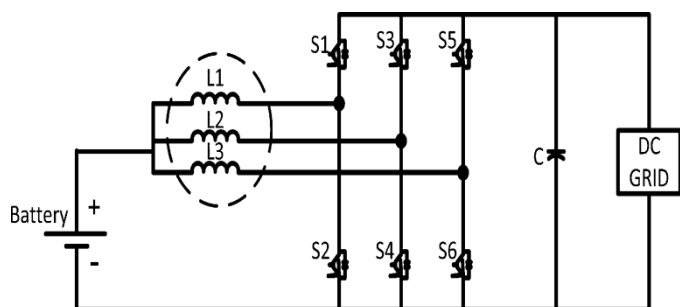


Fig.3. Circuit with Switch 2 and Switch 5 in State 2 for V2G boost or G2V buck operation with vehicle side inductors interleaved.

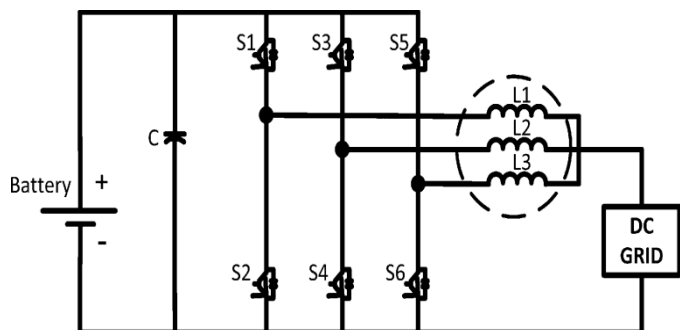


Fig.4. Circuit with Switch 3 and Switch 4 are in State 1 for V2G buck or G2V boost operation with dc grid side inductors interleaved.

When the converter is to connect to a dc grid, Switch 4 will be in State 1 to isolate from the ac grid. Fig. 2 shows the OFF condition where all the switches are in State 1; in this situation, there will be no power transfer. From Fig. 3, it can be observed that for V2G boost operation, the interleaved technique can be applied on the battery side

stresses.

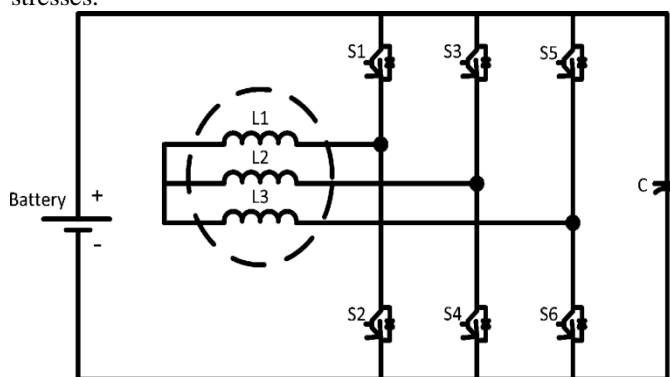


Fig.5.circuit with switch 1 is in state 2 for traction mode operation

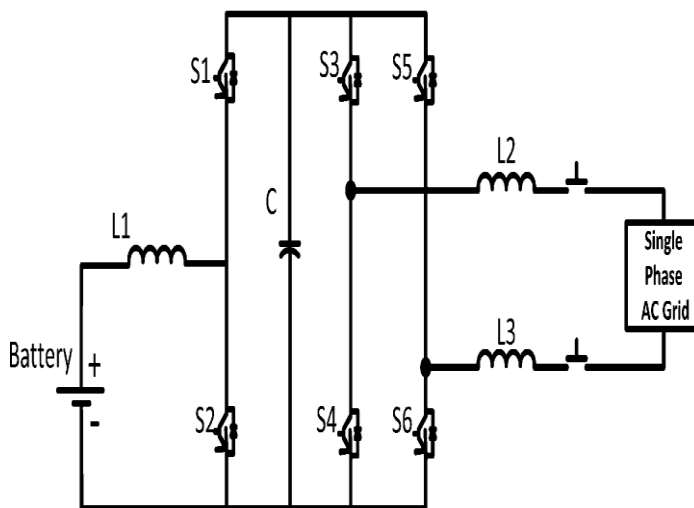


Fig.6. Circuit configuration for bidirectional interface with a single-phase ac grid.

This converter can be used for bidirectional power transfer

Between a single-phase ac grid and the vehicle battery. For this configuration, Switch 1 and Switch 5 are kept in State 1, while all switches are to be in State 2. The two phases of traction motor windings are connected with the single-phase ac grid side and another switch connects with battery as shown in fig.6.

Operating mode 1 in Fig. 3 and operating mode 2 in Fig. 4 Have been verified in simulation. Operating mode 1 is experimentally verified using two types of machines. Although, operating mode 2 in Fig. 4 is different from operating mode 1, the converter is symmetrical for these two modes and for experiments they are similar. Therefore, verifying operating mode 1 experimentally is sufficient for both modes. The operation mode in Fig. 5 is the typical traction machine operation which is used in the motor drives of electric and hybrid vehicles.

TABLE 2  
PARAMETER SPECIFICATION FOR ANALYSIS

<b>Input voltage range</b>	100V-250V
<b>Maximum output voltage</b>	650V
<b>Machine phase inductance</b>	4.98mH
<b>Output capacitance</b>	3300uF
<b>Load resistance</b>	20ohm
<b>Maximum input current</b>	30A

The machine inductance would be suitable for all the operating modes, since it is just the configuration of the winding of the machine, and the machine inductances are typically large values. The performance depends on the machine specifications. The maximum current limit is within the thermal limit of the machine, and the ripple current is indicated by the fixed inductance of the machine as the machine windings cannot be changed. The bus capacitor is selected to handle the voltage ripple and the appropriate switching frequency is selected beyond the acoustic range of frequencies.

### III. SIMULATION RESULTS

In automotive applications, different kinds and ratings of electric machines are used. The applicability of the concept on different electric machines used in automotive applications is tested with simulation models that would provide the most realistic predictions.

#### A. Coupled Simulation With PMSM

The concept has been verified with a small sized three-phase, 500 W and surface mount PM machine. The machine has 9 slots and 6 poles. This machine has been integrated with the converter for the same converter topology given in Fig. 3. The simulation parameters are: battery voltage 12 V, output reference voltage 18 v, and load resistance 0.5  $\Omega$ .

Fig. 7 shows that the output voltage settles at the reference voltage of 18 V. The converter currents in the interleaved machine coil windings are shown in Fig. 8; the current ripple is high in these windings since the machine winding inductance is low.

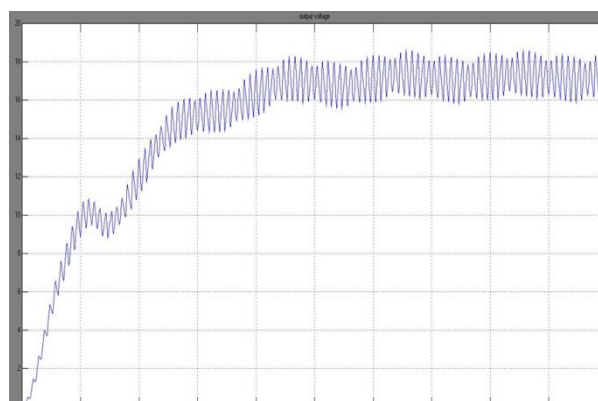


Fig.7.DC output voltage from coupled simulation

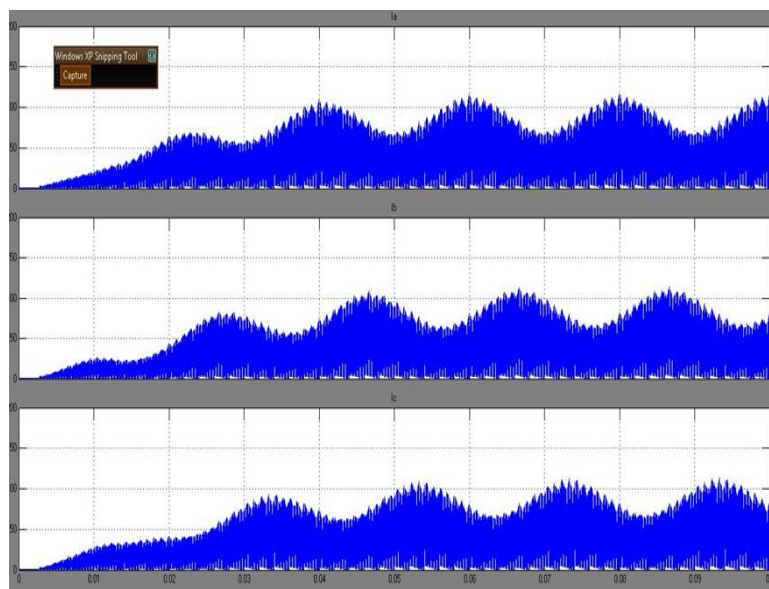


Fig.8. Phase currents in the three windings of the machine from coupled simulation.

#### B. Simulation with an Induction Machine

An induction machine is also a common type of electric machine type used in traction applications. A 10 HP, three-phase induction machine where the neutral point is available has been chosen as a traction machine for experimental verification. Dynamic simulation using MATLAB/Simulink has been done with the inductances of the machine windings. The power transfer characteristics and the interleaving technique for distributing the input currents into the three-phase windings can be analyzed with this simulation.

1) *Mode 1 and Mode 2 Simulation:* Mode 1 is for power flow From the battery to the dc grid and Mode 2 is for power flow From the dc grid to battery. In the simulation, three inductors With the same values of the winding inductance of the induction machine have been used to build the converter as the topology of Fig. 3 for V2G boost mode of operation. The simulation block diagram is shown in Fig. 9(a). The simulation for V2G buck mode of operation using the configuration of Fig. 4 has been also done; the simulation block diagram for this mode is shown in Fig. 10(b).

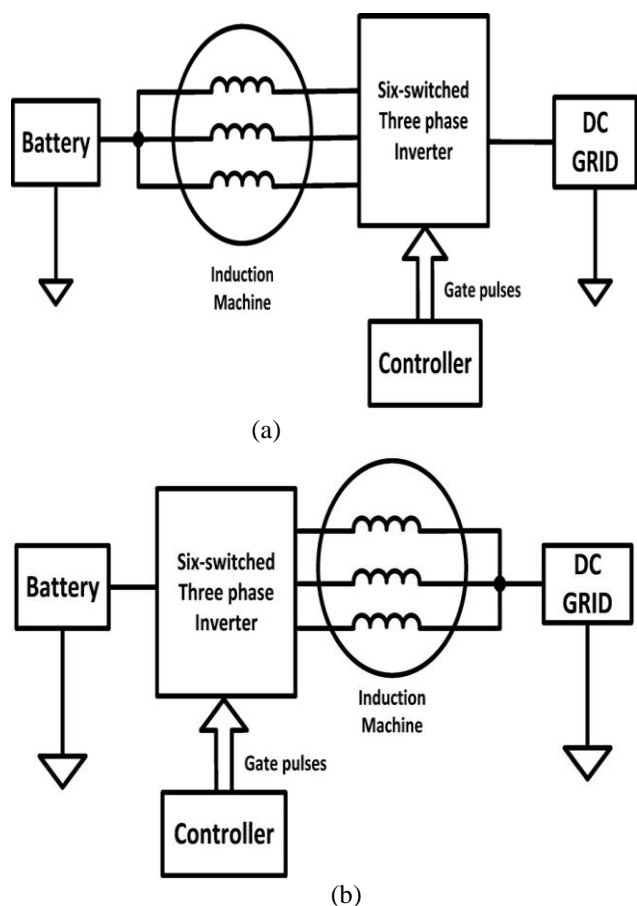
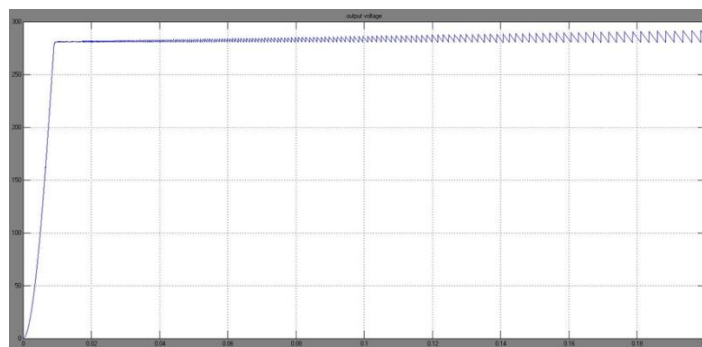
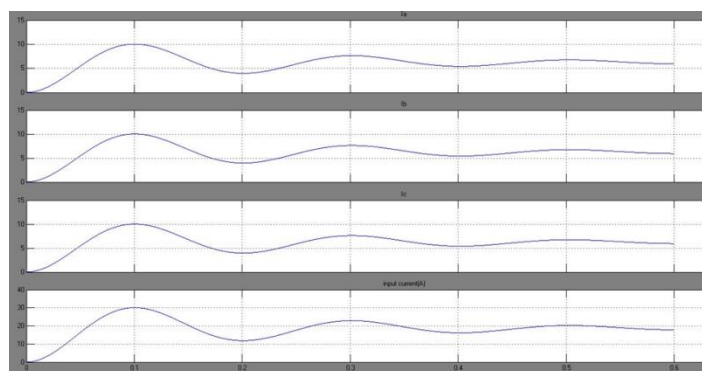


Fig.9. Integrated converter and induction machine operation with dc grid;(a) V2G boost mode of operation and (b) V2G buck mode of operation.

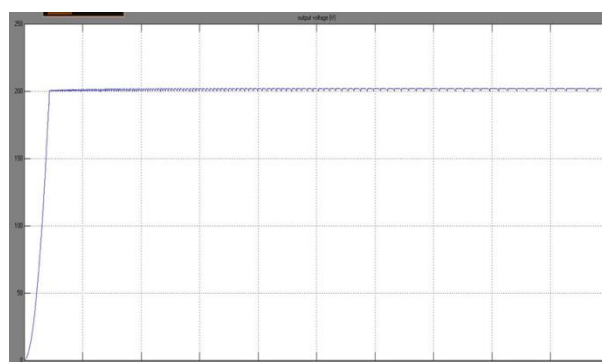


10(a)

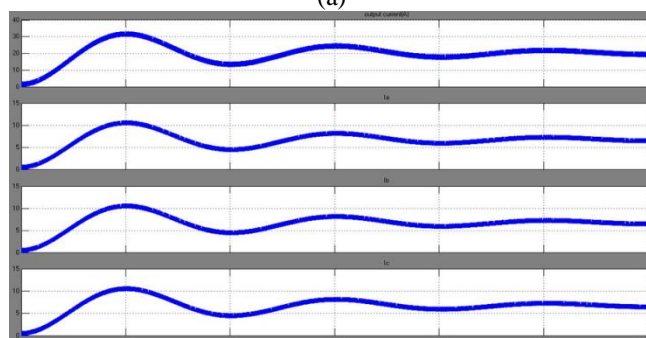


(b)

Fig.10. (a) output voltage (b)input current and shared currents in 3-ph windings of the induction machine for boost mode.



(a)



(b)

Fig.11. (a) output voltage (b)output current and shared output currents in 3-ph windings of the induction machine for buck mode.

The simulation parameters for boost operation are: input voltage is 200 V, output reference voltage is 260 V, maximum input current limit is 30 A, induction machine phase inductance is 5mH, output capacitor is 3300 $\mu$ F, load resistance is 20  $\Omega$ , and PWM switching frequency is 20 kHz. From the simulation result shown in Fig. 10(a), it is observed that the output voltage is following the reference voltage of 260 V in the boost mode of Fig. 3. The simulation parameters for buck operation are: input voltage is 400 V, output reference voltage is 200 V, maximum input current limit is 30 A, induction machine phase inductance is 5mH, load resistance is 10  $\Omega$ , and PWM switching frequency is 20 kHz. From the simulation result shown in Fig. 11(b), it is observed that the output voltage is following the reference voltage of 200 V in the buck mode of Fig. 4.

In the case of boost operation, the output power level is 4 kW. The interleaving technique has been applied in the battery side of the system as shown in Fig. 3 and Fig. 9(a). The results in Fig. 11(b) show that the input current can be equally shared through the windings of the three-phase induction machine.

In the case of buck operation, the interleaving technique has been applied in load side of the system shown in Fig. 4 and Fig. 9(b). The results in Fig. 11(b) show that the output current can be equally shared through the windings of the three-phase induction machine.

**2) Mode 4 and Mode 5 Simulation:** Mode 4 and Mode 5 allow power flow from the battery to a single phase ac grid and from a single phase ac grid to battery, respectively. In the simulation, three inductors of the same values as that of the induction machine have been used in the topology of Fig. 6. The simulation models for Mode 4 and Mode 5 are given in Fig. 12(a) and (b). For power transfer between the battery and an ac grid, the converter is configured in two stages with a dc/dc converter using one phase leg followed by an H-bridge inverter that interfaces with the ac grid (see Fig. 6). A single phase PLL algorithm has been developed to synchronize the inverter with the single phase grid. In the PLL algorithm, the grid voltage is first shifted by 90 $^\circ$  and then  $dq$ -transformation on the grid and the shifted voltages gives the  $d$ -axis and  $q$ -axis voltages. To lock the phase, the  $q$ -axis voltage has been kept at zero by using a loop filter. The converter is operated in the current controlled mode when interfaced with the grid. Current regulation in the  $dq$  domain has been used in the grid connected mode using grid current feedback converted to  $dq$  current [14]. The amount of power transferred from grid to vehicle and V2G depend on the  $i_d$  and  $i_q$  current commands. The current regulator design is based on the following dynamic equations:

$$V_d(t) = R i_d(t) + L \frac{di_d(t)}{dt} - \omega L i_q(t) + e_d(t)$$

$$V_q(t) = R i_q(t) + L \frac{di_q(t)}{dt} - \omega L i_d(t) + e_q(t)$$

Fig. 13(a) and (b) shows the grid voltage and grid current in Mode 4 with a current command  $i_d$  of 30 A and  $i_q$  of zero. In

This case, the power is being transferred from the vehicle to the single-phase ac grid. The power transferred and the grid currents for different current commands  $i_d$  are given in Table 3. single-phase ac grid. The power transferred and the grid currents for different current commands  $i_d$  are given in Table 3.

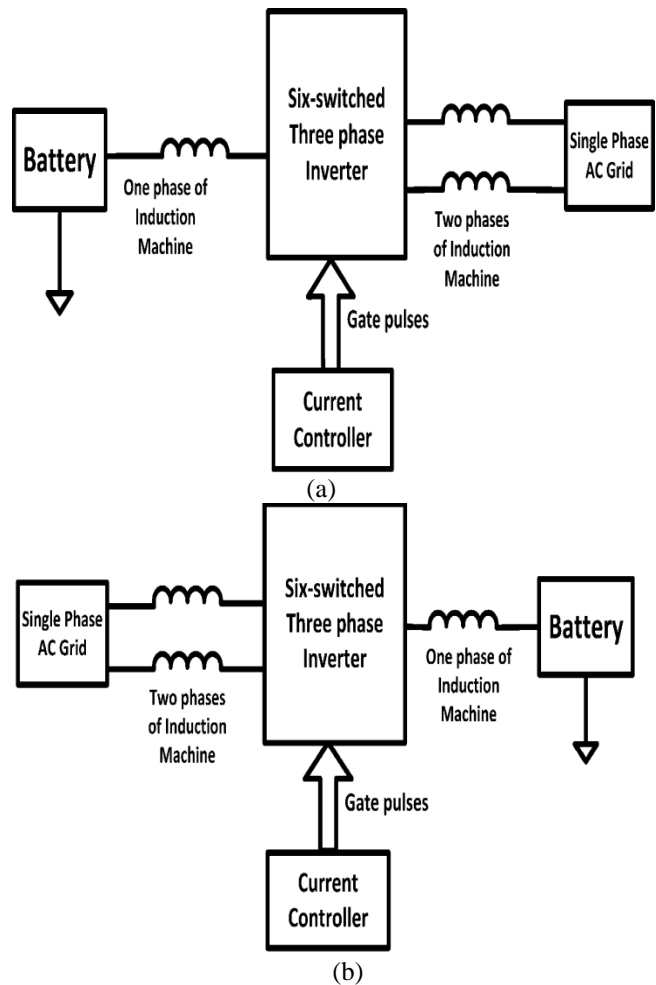


Fig.12. Power flow between the battery and an ac grid: (a) from battery to ac grid (Mode 4), and (b) from ac grid to battery (Mode 5).

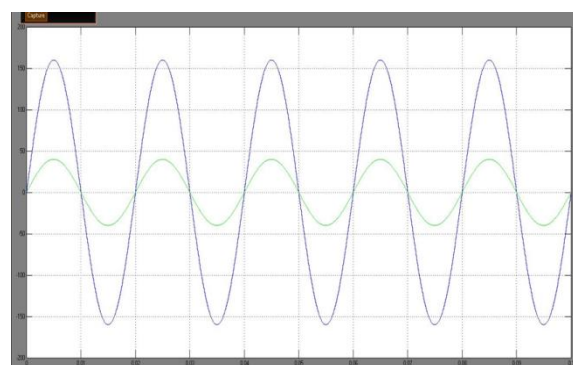


Fig.13 (a). Voltages and currents in Mode 4: (a) grid voltage and grid current.

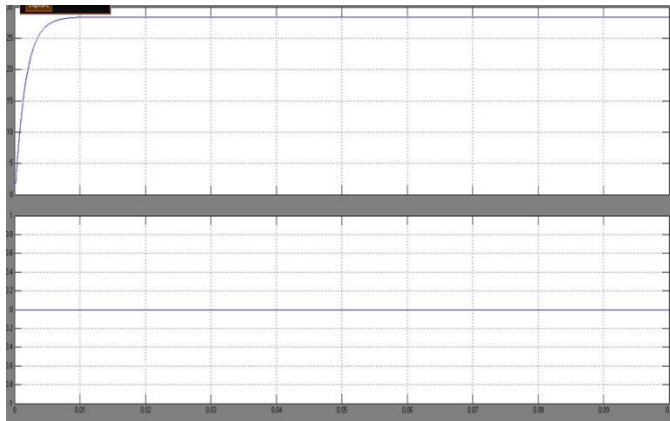


Fig.13(b).command  $i_d$  and  $i_q$  currents.

TABLE 3

POWER FLOW AT DIFFERENT LEVELS IN MODE 4

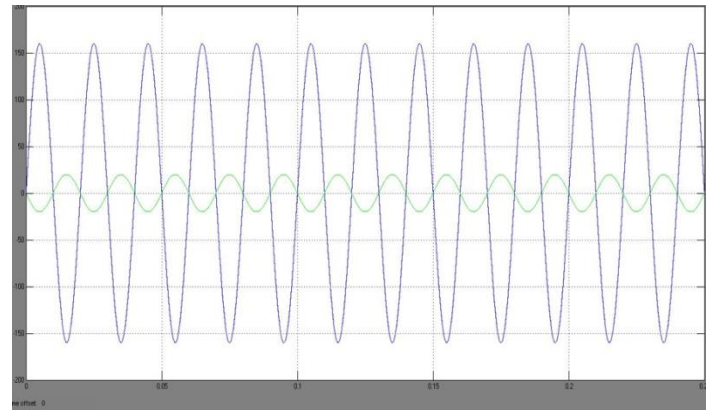
$I_d$ (A) command	$V_{grid}$ (RMS)	$I_{grid}$ (RMS)	Active Power(W)
10	120	7.19	863
15	120	10.52	1262
20	120	14.32	1723
25	120	17.82	2138
30	120	21.16	2540

Fig. 14(a) and (b) shows the grid voltage and grid current in Mode 5; in this case, the current command  $i_d$  is  $-30$  A and  $i_q$  is zero. Power is being transferred from the single-phase ac grid to the vehicle. The power transferred to the battery and the grid currents for different current commands  $i_d$  are given in Table 4.

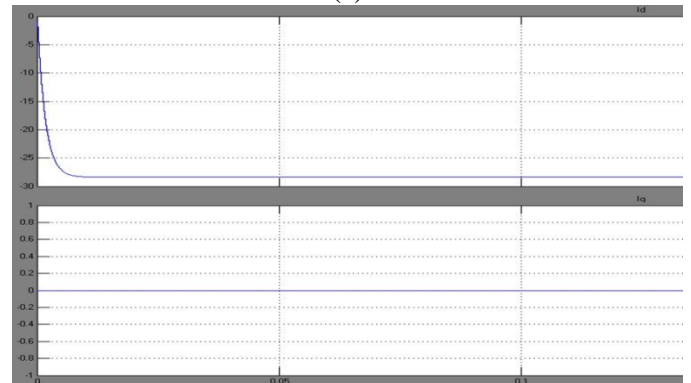
TABLE 4

POWER FLOW AT DIFFERENT LEVELS IN MODE 5

$I_d$ (A) command	$V_{grid}$ (RMS)	$I_{grid}$ (RMS)	Active Power(W)
-10	120	7.14	857
-15	120	10.6	1272
-20	120	14.29	1715
-25	120	17.68	2122
-30	120	21.29	2555



(a)



(b)

Fig.14 (a) grid voltage and current (b) command  $i_d$  and  $i_q$  currents in mode 5.

C. simulation of Fuel cell converter topology:

FUEL CELL (FC) technologies are expected to become an Attractive e power source for automotive applications because of their cleanness, high efficiency, and high reliability.

Although FC systems exhibit good power capability during steady-state operation, the dynamic response of FCs during transient and instantaneous peak power demands is relatively slow. Therefore, the FC system can be hybridized with energy storage systems (ESS) (e.g., batteries or super capacitors) to improve the performance of the FC system during transient and instantaneous peak power demands of a hybrid electric vehicle (HEV).

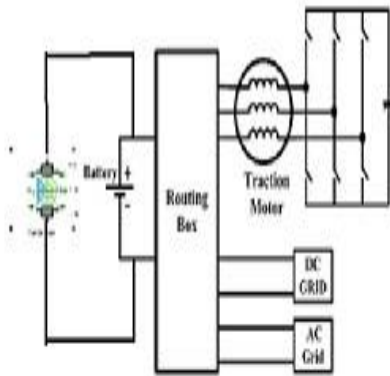


Fig.15.Proposed Fuel Cell Converter Topology

Fig. 15 shows the proposed converter topology, Here we are hybridizing fuel cell with the energy storage system, this combination increases the performance of the system and also we get high efficiency. The simulation parameters for boost operation are input voltage 12V, output reference voltage is 18V, and induction machine phase inductance is 5 mH, load resistance 0.5Ω, output capacitance 3300μF.

Here we are using fuel cell of 1.26KW, 24V, and stack efficiency of 46%.

Fig.16 shows the simulation diagram of fuel cell converter topology in the boost mode and the output voltage and shared input currents in the 3-phases are shown in fig. 17 & 18. From figure 17, we can observe that the output voltage is following the reference voltage of 18V.

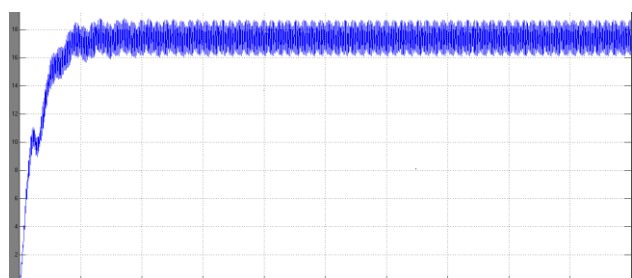


Fig. 17 output voltage in boost mode for proposed fuel cell converter topology.

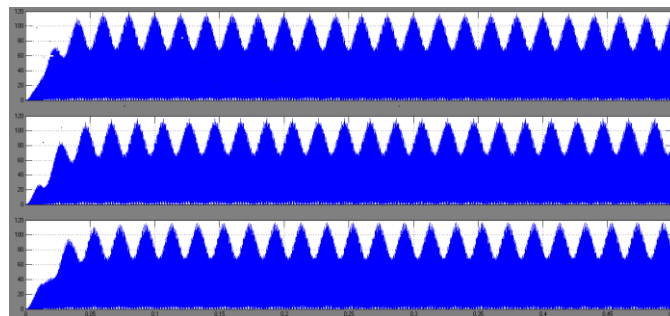


Fig.18 input currents in the three phase windings of induction machine in proposed converter topology.

#### IV. CONCLUSION

In this paper, a new fuel cell converter topology has been proposed in order to optimize the drive system that uses interleaving technique and phase windings of motor to power transfer. The converter reconfiguration concept is useful in minimizing the size and parts in the powertrain of an electric vehicle. The machine-converter coupled simulation results showed that the integrated converter can be used for the power transfer with versatility without significantly extra power elements. The simulation results are done for V2G boost mode. It can be verified that the proposed converter topology can work efficiently in V2G boost mode.



## V. REFERENCES

- [1] S. Lacroix, E. Laboure, and M. Hilaiet, "An integrated fast battery charger for electric vehicle," in *Proc. IEEE Veh. Power and Propulsion Conf.*, Oct. 2010, pp. 1–6.
- [2] M. Milanovic, A. Roskaric, and M. Auda, "Battery charger based on double-buck and boost converter," in *Proc. IEEE Int. Symp. Ind. Electron.*, Jul. 1999, vol. 2, pp. 747–752.
- [3] A. G. Cocconi, "Combined motor drive and battery recharge system," U.S. Patent 5 341 075, 23 Aug. 1994.
- [4] S. K. Sul and S. J. Lee, "An integral battery charger for four-wheel drive electric vehicle," *IEEE Trans. Ind. Appl.*, vol. 31, no. 5, pp. 1096–1099, Sep./Oct. 1995.
- [5] D. Thimmesch, "An SCR inverter with an integral battery charger for electric vehicles," *IEEE Trans. Ind. Appl.*, vol. IA-21, no. 4, pp. 1023–1029, Jul./Aug. 1985.
- [6] L. Solero, "Nonconventional on-board charger for electric vehicle propulsion Batteries," *IEEE Trans. Veh. Technol.*, vol. 50, no. 1, pp. 144–149, Jan. 2001.
- [7] S. Haghbin, S. Lundmark, M. Alak'ula, and O. Carlson, "An isolated high Power integrated charger in electrified vehicle applications," *IEEE Trans. Veh. Technol.*, vol. 60, no. 9, pp. 4115–4126, Nov. 2011.
- [8] G. Pellegrino, E. Armando, and P. Guglielmi, "An integral battery charger With Power Factor Correction for electric scooter," in *Proc. IEEE Electric Mach. Drives Conf.*, May 2009, pp. 661–668.
- [9] N. M. L. Tan, T. Abe, and H. Akagi, "A 6-kW, 2-kWh Lithium-Ion battery Energy storage system using a bidirectional isolated DC-DC converter," in *Proc. Power Electron. Conf.*, Jun. 2010, pp. 46–52.
- [10] S. Dwari and L. Parsa, "An efficient high-step-up interleaved DC-DC Converter with a common active clamp," *IEEE Trans. Power Electron.* vol. 26, no. 1, pp. 66–78, Jan. 2011.
- [11] O. Hegazy, J. Van Mierlo, and P. Lataire, "Analysis, modeling, and implementation of a multidevice interleaved DC/DC converter for fuel cell Hybrid electric vehicles," *J. Power Electron.*, vol. 27, pp. 4445–4458, Jul. 2011.
- [12] O. Hegazy, J. Van Mierlo, and P. Lataire, "Control and analysis of an integrated bidirectional DC/AC and DC/DC converters for plug-in hybrid electric vehicle applications," *J. Power Electron.*, vol. 11, no. 4, pp. 408–417, Jul. 2011.
- [13] O. Ellabban, O. Hegazy, J. Van Mierlo, and P. Lataire, "Dual loop digital control design and implementation of a dsp based high power boost converter in fuel cell electric vehicle," in *Proc. IEEE Int. Conf. Optim. Electr. Electro. Equipment*, May 2010, pp. 610–617.
- [14] M. N. Arafat, S. Palle, Y. Sozer, and I. Husain, "Transition control strategy between standalone and grid-connected operations of voltage-source inverters," *IEEE Trans. Ind. Appl.*, vol. 48, no. 5, pp. 1516–1525, Sep./Oct. 2012.

## AUTHOR'S PROFILE



### P. Sandhya

Received the B.Tech degree in Electrical and Electronics Engineering From nagarjuna Institute of science and technology, mlg, India in 2012 and at present Pursuing M. Tech with the Specialization of Power Electronics and Electric Drive in Anurag Engineering college Kodad.



### D. Pomya

Graduated in EEE from anurag engineering college 2007. He received M.E degree Electronics in osmania university Hyderabad in 2009, Presently working as Assistant Professor Anurag Engineering college. kodad